Chiral spin currents in a trapped-ion quantum simulator using Floquet engineering

Tobias Graß, Alessio Celi, Guido Pagano, and Maciej Lewenstein

Phys. Rev. A **97**, 010302 — Published 19 January 2018

DOI: 10.1103/PhysRevA.97.010302

Chiral spin currents in a trapped-ion quantum simulator using Floquet engineering

Tobias Graß[1], Alessio Celi[2], Guido Pagano[1], Maciej Lewenstein[2,3]
[1] *Joint Quantum Institute, University of Maryland, College Park, MD 20742, U.S.A.*
[2] *ICFO-Institut de Ciències Fotòniques, The Barcelona Institute of Science and Technology, 08860 Castelldefels, Spain and*
[3] *ICREA, Psg. Lluís Companys 23, 08010 Barcelona, Spain*

The most typical ingredient of topologically protected quantum states are magnetic fluxes. In a system of spins, complex-valued interaction parameters give rise to a flux, if their phases do not add up to zero along a closed loop. Here we apply periodic driving, a powerful tool for quantum engineering, to a trapped-ion quantum simulator in order to generate such spin-spin interactions. We consider a simple driving scheme, consisting of a repeated series of locally quenched fields, and demonstrate the feasibility of this approach by studying the dynamics of a small system. An emblematic hallmark of the flux, accessible in experiments, is the appearance of chiral spin currents. Strikingly, we find that in parameter regimes where, in the absence of fluxes, phonon excitations dramatically reduce the fidelity of the spin model simulation, the spin dynamics remains widely unaffected by the phonons when fluxes are present. Our work provides a realistic experimental recipe to engineer the minimal building block of a topological quantum system with currently existing ion traps apparatus.

Magnetic fluxes can profoundly alter the behavior of a quantum system. They are responsible for the Aharonov-Bohm effect [1, 2], fractal energy spectra [3, 4], or intriguing many-body phases exhibiting fractional quantum Hall physics [5, 6]. Most importantly, properties of a quantum system can be topologically protected in the presence of fluxes, as is the case for quantized Hall conductances. The underlying mechanism is due to breaking of time-reversal symmetry (TRS) which fixes the chirality of the edge currents. Thereby, suppressed backscattering leads to quantized conductances. An exciting application of topological protection is fault-tolerant quantum computing [7]. In the present paper we will show that a magnetic flux can enhance the fidelity of a quantum simulation even in the few-body regime.

Quantum simulation of topological matter has been pursued very actively using cold atoms [8–14], photons in cavities [15–18], or nitrogen-vacancies [19]. Another experimental platform with long-standing history of quantum simulations involves trapped ions: Refs. [20, 21] suggested the implementation of spin models, which have later been realized in the laboratory using linear Paul traps [22–26], or two-dimensional Penning traps [27, 28]. Nowadays trapped ions are the leading platform for quantum simulation of spin models [29]. They offer high-efficiency detection and ion addressability at the single-site level [30, 31], enabling full state tomography [32] and measurement of high-order N-body correlators [33].

A particularly interesting feature of trapped ions are long-range spin-spin interactions, which can be exploited to engineer magnetic fluxes even in a 1D architecture [34]. A standard route to artificial fluxes is Floquet engineering, that is the control of a Hamiltonian via periodic driving. Early proposals for modifying the tunneling strength in quantum wells using time-periodic fields date back to the 1980s and 1990s [35–38]. Since then the progress in laser cooling and the emergence of cold atoms as highly controllable quantum systems have provided an experimental platform to apply these ideas. Controlling the tunneling of atoms in an optical lattice by periodic modulation was proposed in Refs. [39, 40] and realized in Refs. [41, 42]. The technique then became a widespread tool for implementing artificial gauge potentials in atomic systems [8, 10, 11, 14]. More generally, Floquet engineering has been recognized as a strategy for producing topological phases of matter such as topological insulators and Majorana fermions [43–45].

In this paper we study the feasibility of Floquet engineering in a system of trapped ions [34, 46, 47]. Similar to the proposal of Ref. [34], we consider a time-periodic series of local quenches, that is, of local potentials being repeatedly switched on and off. On the level of a spin system, it has been demonstrated in Ref. [34] that such shaking is able to equalize all interaction strengths, and to render interaction parameters complex-valued. In large enough systems, of the order of hundreds of spins, this has been shown to give rise to a fractal energy spectrum with end states between different energy bands. In the present paper, we are interested in *microscopic* signatures of complex-valued spin-spin interactions, having direct relevance for trapped ions experiments. To this end, we consider a minimal system of three ions in a linear Paul trap, which we realistically describe by a spin-phonon (or Dicke) model rather than by a pure spin model. Our simulation identifies a parameter regime for which Floquet engineering is feasible: On the one hand, the shaking has to be fast compared to the spin dynamics in order to achieve the desired Floquet Hamiltonian, on the other hand, the shaking must be slow compared to the spin-phonon coupling such that vibrational and spin degrees of freedom remain decoupled. Then, the system reduces effectively to the one of a single particle hopping along a triangle pierced by a magnetic flux, and chiral currents appear as an immediate consequence of the flux. Unexpectedly, our simulation also reveals that phonon effects, which reduce the fidelity of the quantum simulation, are suppressed through the presence of magnetic fluxes. It remains an interesting open question

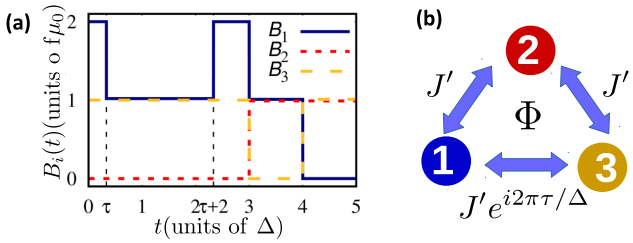

FIG. 1. Driving scheme. (a) Shaking protocol for a chain of three spins: The first sequence ($t < 3$) renders interactions between spin 1 (left ion) and 3 (right ion) complex-valued. For $3 < t < 4$ and $4 < t < 5$ real-valued interactions between spin 1 and 2 (center ion), and 2 and 3 are acquired. The strength of nearest-neighbor interactions is suppressed by a factor 1/5, while second-neighbor interactions are suppressed by a factor 2/5. This allows to obtain a situation as depicted in (b): All ions interact equally, encircling a magnetic flux Φ.

whether this behavior can be traced back to the topological protection expected for larger-sized chiral systems.

We start from a Dicke-like Hamiltonian given by

$$H_0(t) = \sum_m \hbar\omega_m a_m^\dagger a_m + \sum_{i,m} \hbar\Omega_i\eta_{i,m}(a_m + a_m^\dagger)\sigma_i^x \sin(\omega t), \tag{1}$$

describing the collective motion of ions in terms of phonons, created by $a_m^\dagger$ at frequencies ω_m, coupled to two internal states of the ions. Here, we work in the (fast) rotating frame of the atomic transition, and apply rotating-wave approximation. Raman lasers with Rabi frequency Ω_i and beatnote frequency ω induce spin flips, described by a Pauli matrix σ_i^x at an individual ion denoted by i, and (de-)excites phonon modes. The strength of this coupling further depends on the Lamb-Dicke parameters $\eta_{i,m}$. The spin degrees of freedom can be decoupled from "dressed" phonon operators [20, 21], and the time evolution is captured by an effective Ising spin model [23, 48], $H_J = \hbar\sum_{ij} J_{ij}\sigma_i^x\sigma_j^x$, with couplings $J_{ij} = \Omega_i\Omega_j\sum_m \frac{\eta_{i,m}\eta_{j,m}}{\delta_m}$, controlled by the detuning $\delta_m = \omega - \omega_m$.

For the shaking, we drive the system with a transverse magnetic field term $H_B(t) = \hbar\sum_i[B_0+\mu_i(t)]\sigma_i^z \equiv H_{B0} + H_{B1}(t)$. The homogeneous and time-independent term H_{B0} provides an approximate XX symmetry to the Ising model. The inhomogeneous time-dependent one, $H_{B1}(t)$ implements the shaking protocol. However, on the level of a spin-phonon model, a transverse field also leads to entanglement between spins and phonons [48, 49].

Noting that $[H_{B0}, H_{B1}] = 0$, we derive an effective Hamiltonian by first switching to the interaction picture of H_{B0} via $U(t) = \exp[-iH_{B0}t]$. Applying the rotating-wave approximation, we get an effective XX model, $U(t)^\dagger H_0(t)U(t) - i\hbar U(t)^\dagger\frac{\mathrm{d}}{\mathrm{d}t}U(t) = H_{XX} + H_{B1}(t)$, with $H_{\mathrm{XX}} = \hbar\sum_{ij} J_{ij}\,\sigma_i^+\sigma_j^- + \mathrm{H.c.}$, where $\sigma^\pm \equiv (\sigma^x \pm i\sigma^y)/2$. Then, we switch to the interaction picture of the time-dependent part H_{B1}, via $\tilde{U}(t) = \exp[-i\sum_i \chi_i(t)\sigma_i^z]$,

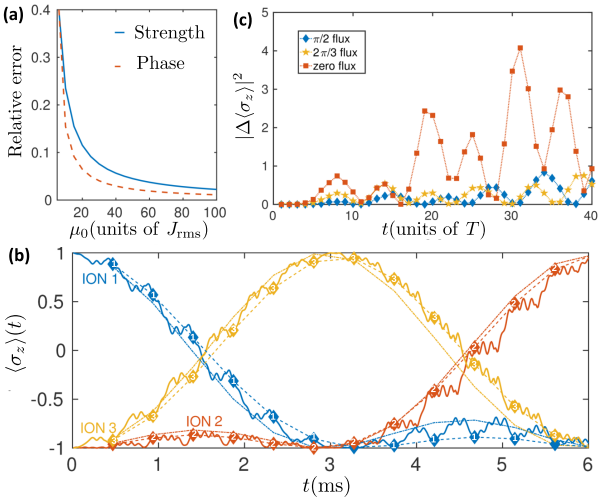

FIG. 2. Fidelity of different descriptions. (a) For $\tau/\Delta = 1/4$, we evaluate the discrepancy between the ideal model as depicted in Fig. 1(b) and the exact Floquet Hamiltonian from the XX model as a function of the driving strength μ_0. (b) We compare the dynamics in the Ising model H_J (three solid lines for three ions, distinguished by color and by the numbers within the diamonds along the lines) and XX model H_{XX} (dashed-dotted lines). The diamonds (connected by dashed lines as a guide to the eye) mark the stroboscopic evolution at times $t = mT$. (c) For different values of the flux and at stroboscopic times $t = mT$, the deviations between Ising and Dicke dynamics is plotted, defined as $|\Delta\langle\sigma_z\rangle|^2 \equiv \sum_i \left(\langle\sigma_z^i\rangle_{\mathrm{Ising}} - \langle\sigma_z^i\rangle_{\mathrm{Dicke}}\right)^2$. Here, as in rest of the paper, the system parameters are $\delta_{\mathrm{COM}} = 2\pi \times 80$ kHz for the blue-detuning from the center-of-mass mode, mass $M = 171$amu, trap frequencies $\omega_{XY} = 2\pi \times 5$ MHz and $\omega_Z = 2\pi \times 900$ kHz. The Rabi frequency is $\Omega = 2\pi \times 200\,$kHz, recoil frequency is $\omega_{\mathrm{rec}} = 2\pi \times 26\,$kHz. This choice leads to a root mean square of the spin-spin interactions $J_{\mathrm{rms}} = 2\pi \times 270$ Hz. Field strengths are $B_0 = J_{\mathrm{rms}}$ and $\mu_0 = 20J_{\mathrm{rms}}$.

where $\chi_i(t) = \frac{1}{\hbar}\int_0^t \mathrm{d}\tau\mu_i(\tau)$. The final Hamiltonian $H'_{XX}(t) = \tilde{U}(t)^\dagger H_{XX}(t)\tilde{U}(t) - i\hbar\tilde{U}(t)^\dagger\frac{\mathrm{d}}{\mathrm{d}t}\tilde{U}(t)$ again has XX structure but with time-dependent couplings. By time-averaging over a period T, we get a time-independent XX Hamiltonian with effective couplings given by [50]

$$J'_{ij} = \frac{J_{ij}}{T}\int_0^T e^{2i[\chi_i(t)-\chi_j(t)]}\mathrm{d}t. \tag{2}$$

We apply this general formalism to a concrete driving scheme, similar to the one proposed in Ref. [34]. Each potential $\mu_i(t)$ takes piecewise constant values, being integer multiples of some frequency $\mu_0 = \pi/\Delta$. Here, Δ provides the time unit, with T an integer multiple of Δ. This choice is motivated in the following way:

1. If two potentials μ_i and μ_j remain constant during an interval Δ, the interaction J'_{ij} remains unchanged if $\mu_i = \mu_j$, or else is fully suppressed: $J'_{ij} = \frac{J_{ij}}{\Delta}\int_0^\Delta \mathrm{e}^{2im\mu_0 t}\mathrm{d}t = J_{ij}\delta_{m,0}$. This feature al-

lows for engineering the effective strength of interactions.

2. If a potential changes within an interval Δ, complex interaction parameters can arise. For concreteness, let us assume that two potentials differ by $m\mu_0$ for a time $\tau = \Delta/q$, with $m \in \mathbb{Z}$. The potentials shall then drop to zero simultaneously for an interval of length Δ, and finally return to their original values for an interval of length $\Delta - \tau$. For such sequence, the first order Floquet analysis yields a phase factor:

$$J'_{ij} = \frac{J_{ij}}{2\Delta}\int_{\tau}^{\tau+\Delta} \mathrm{e}^{2\pi i m/q}\mathrm{d}t = \frac{J_{ij}}{2}\mathrm{e}^{2\pi i m/q}. \qquad (3)$$

Accordingly, the shaking period shown in Fig. 1(a) should (i) generate a complex phase $\varphi/(2\pi) = -\tau/\Delta$ on the link between spin 1 and 3, and (ii) enhance the ratio $|J'_{13}|/|J'_{12}| = |J'_{13}|/|J'_{23}|$ by a factor 2 compared to the original ratio $|J_{13}|/|J_{12}|$. This can fully compensate the decay of interaction strength with distance, and lead to approximately equal interactions between all pairs, cf. Fig. 1(b).

The reasoning so far was based on the assumption that time-averaging in the interaction picture approximates well the effective Hamiltonian. Rigorously, the effective Hamiltonian is obtained from Floquet's theorem. Due to time-periodicity of the evolution operator $U(t, t_0) = U(t + T, t_0 + T)$, the operator $U(T, 0)$ fully determines the evolution at stroboscopic times $t = mT$. Writing $U(T, 0) = \exp\left(-\frac{i}{\hbar}H_{\mathrm{eff}}T\right)$, we obtain an effective Hamiltonian H_{eff}, which exactly describes the stroboscopic dynamics. For our protocol, consisting only of quenches, H_{eff} can straightforwardly be evaluated. As seen in Fig. 2(a), the discrepancy between the couplings in the exact H_{eff} and the couplings approximated according to Eq. (2), regarding both absolute value and phase, decreases as $\sim 1/\mu_0$ with the shaking strength. Relative errors < 0.1 require a shaking $\mu_0 \approx 20 J_{\mathrm{rms}}$, where J_{rms} denotes the root mean square of the spin-spin interactions before shaking.

Fig. 2(b) compares the spin dynamics in the Ising and the XX model in the presence of a flux $\Phi = \pi/2$ ($\tau = \Delta/4$) after initially preparing the system in a state $|\uparrow\downarrow\downarrow\rangle$. With $B_0 = J_{\mathrm{rms}}$, the curves show good quantitative agreement. Small wiggles in the dynamics of the Ising model are due to the strong transverse fields, but do not appear in the stroboscopic evolution. Both models exhibit clear evidence of a chiral current, as the up-spin moves counter-clockwise from ion 1, to ion 3, and finally to ion 2. Notably, the evolution is almost periodic with a period T', so comparing the states at time t and $T' - t$ allows for a practical detection of TRS breaking [17].

These results establish that Floquet engineering works sufficiently well for an effective Ising system, if shaking strength $\mu_0 \sim 10$ kHz is at least an order of magnitude faster than the spin interactions ($J \sim 1$ kHz before shaking, $J' = J/5 \sim 200$ Hz after shaking). However, the validity of the spin model description also requires the detuning of the spin-phonon coupling to be fast. A realistic choice is $\delta \sim 100$ kHz, i.e. one order of magnitude above μ_0. To explicitly check the role played by phonons we have simulated the dynamics under the Dicke Hamiltonian $H(t) = H_0(t) + H_B(t)$ using Krylov methods. The results are seen in Fig. 3 for different fluxes. We first note that the evolution for $\Phi = \pm\frac{\pi}{2}$, shown in panels (a,b), exhibits TRS breaking in the same way as discussed before for the pure spin model. As expected, the direction of the spin current depends on the sign of the flux. For other fractional values of the flux, such as $\Phi = 2\pi/3$ shown in panel (c), the evolution is not periodic on relevant time scales, but breaking of TRS can still be inferred from obvious differences between clockwise and counter-clockwise flow. In contrast, for "integer" fluxes (i.e. $\mathrm{mod}(\Phi, \pi) = 0$) shown in panel (d), the spin initially flows clockwise and counter-clockwise at equal rate.

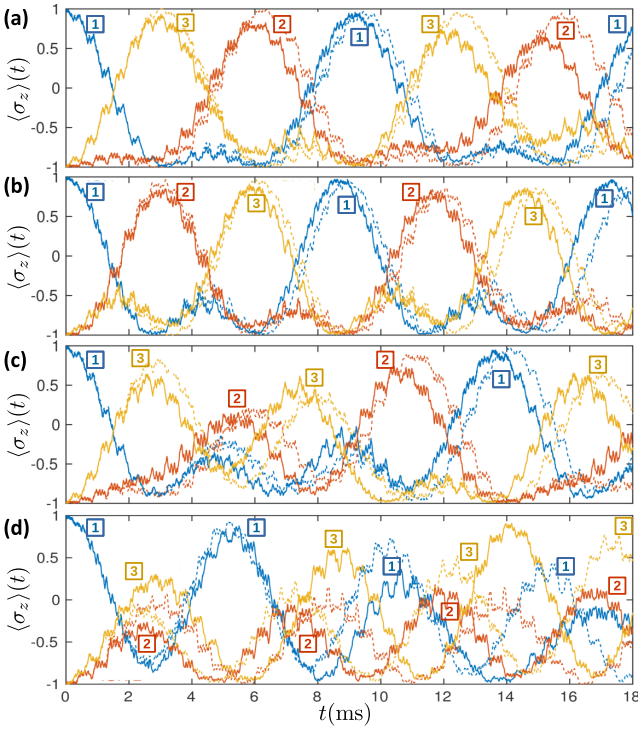

FIG. 3. Comparison between spin model dynamics and Dicke model dynamics. We plot the spin evolution in the Dicke model (solid lines) and the Ising model (dashed lines) for different parameters τ, adjusting fluxes $\Phi = 2\pi\tau/\Delta$: (a) $\tau = \Delta/4, \Phi = \frac{\pi}{2}$. (b) $\tau = 3\Delta/4, \Phi = -\frac{\pi}{2}$. (c) $\tau = \Delta/3, \Phi = \frac{2\pi}{3}$. (d) $\tau = \Delta, \Phi = 0$. In each plot, the different ions are distinguished by different colors and boxed numbers next to the lines.

Strikingly, TRS breaking stabilizes the quantum simulation. For fractional fluxes [panel (a–c)], the evolution in the Dicke model agrees well with the Ising model dynamics. In contrast, the spin dynamics with integer fluxes [panel (d)] is heavily perturbed by the phonons, although only a single parameter τ is changed, see also Fig. 2(c)

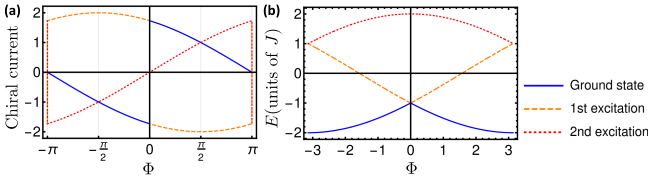

FIG. 4. Chiral currents and energy spectrum. For a particle on a triangle with $|J_{ij}| = J$ and flux Φ, we plot (a) the chiral currents defined in Eq. (4), and (b) the eigenenergies, in units of J, as a function of the flux.

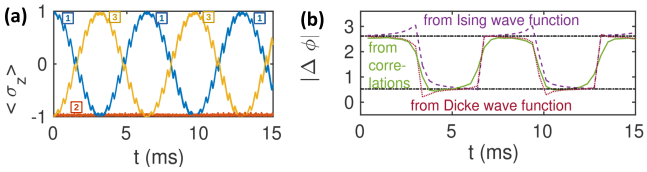

FIG. 5. Phase measurement. (a) Spin evolution for shaking on the first and the third ion ($\mu_0 = 10 J_{\rm rms}$), with the central ion detuned at any time, having perfect agreement between Dicke and Ising model dynamics. Different ions are distinguished by color and boxed number along the curves. (b) The complex phase is extracted from the wave function dynamics in the Ising and the Dicke model, and from the correlation functions in the Dicke model. Theoretically expected values, for $\tau = \Delta/3$, are marked by the black dash-dotted lines.

where the corresponding error is plotted as a function of time. This effect can not be traced to the number of phonons which is approximately the same for different τ. With a variety of simulations we checked that this protective effect is not an accidental one: We varied different system parameters (magnetic field strength, shaking period, Rabi frequency), we changed the gauge of our shaking scheme, or we started our time evolution from different initial states (not restricted to phonon vacua). In all cases, we observed the protective role apparently played by the flux. We have also carried out analog simulations for a system of four ions, forming two triangles glued together. Also here the synthetic flux was found to protect the spin dynamics, but the effect is less pronounced than for three ions. Interestingly, for four ions the presence of the flux also does not fully restrict the spin flow to one direction, suggesting that chirality of the flow and protection against phonons are linked.

So far, we have studied the dynamics of a system initially prepared out of equilibrium. Quantum revivals of the initial state allowed for demonstrating TRS breaking. The length of a revival period generally depends on the ratios of energy gaps between contributing eigenstates. As seen in the energy spectrum in Fig. 4(b), only a single energy difference characterizes the spectrum of a triangle at (half-)integer flux, guaranteeing short revival periods. However, other (potentially incommensurate) gap ratios can make revival periods arbitrarily long, as can happen for other fluxes [cf. $2\pi/3$-flux in Fig. 3(c)] or in larger systems. In such cases, a more general criterion for TRS breaking and chirality is required. One possibility is to consider equilibrium chiral currents, quantified as [17]

$$I_{\rm chiral} = i \langle \Psi | \sum_{i \neq j} J_{ij} \sigma_i^+ \sigma_j^- - \text{H.c.} \, | \Psi \rangle \,, \qquad (4)$$

for an eigenstate $|\Psi\rangle$. As seen in Fig. 4(a), at non-integer flux equilibrium chiral currents are non-zero for any eigenstate. At integer flux, chiral currents are zero for non-degenerate eigenstates, or add up to zero for degenerate eigenstates.

Next, we show, for a slightly simplified setting, how to extract the value of the synthetic flux from a spin-spin correlation function. Therefore, we consider a shaking protocol of period $T = 2\Delta$, with $\mu_2 = 2\mu_0$ always detuned from μ_1 and μ_3 which are both set to zero for $\tau < t \leq \tau + \Delta$, while taking values zero and μ_0 at other times. This protocol leads to particularly simple dynamics, as it freezes out the center spin. Thus, with $|\text{L}\rangle$ ($|\text{R}\rangle$) denoting the position of the up-spin at both ends, we obtain a two-level or double-well system described by $H_2 = 2\hbar J'_{13} |\text{L}\rangle \langle \text{R}| + \text{H.c.}$ Accordingly, as seen in Fig. 5(a), the spin dynamics reduces to Rabi oscillations between the left and the right spin with a period $T_{\rm osc} = \pi/|J'_{13}|$. The complex phase φ of J'_{13} is reflected in the relative phase between the two levels. An initial state $\Psi(0) = |\text{L}\rangle$ will evolve to $\Psi(t) = \cos(2|J_{13}|'t) \, |\text{L}\rangle + \exp\left[-i\left(\varphi - \frac{\pi}{2}\right)\right] \sin(2|J_{13}|'t) \, |\text{R}\rangle$, where φ is the complex phase of J'_{13}. Thus, information about the phase is contained in the phase difference $\Delta\phi$ between the two components of the wave function. During the course of time, $\Delta\phi$ is expected to jump between constant values $\Delta\phi_0 = -\frac{\pi}{2} + \varphi = -\pi\left(\frac{1}{2} + \frac{2\tau}{\Delta}\right)$, when $\sin(2|J_{13}|'t)$ and $\cos(2|J_{13}|'t)$ have equal signs, and $\Delta\phi_\pm = \Delta\phi_0 \pm \pi$, if signs are opposite.

The relative phase $\Delta\phi$ can be extracted (up to a sign) from a $\sigma_1^x \sigma_3^x$ measurement. Denoting $\Psi = c_{\rm L} |\text{L}\rangle + c_{\rm R} |\text{R}\rangle$ we have $|\Delta\phi| = \arccos\left(\frac{\langle \sigma_1^x \sigma_3^x \rangle}{2|c_{\rm L}| \cdot |c_{\rm R}|}\right)$, where $|c_{\rm L,R}| = \sqrt{\frac{1}{2}\left(1 \pm \langle \sigma_1^z \rangle\right)}$. In Fig. 5(b), we plot $\Delta\phi$, as measured in three different ways: (i) from the wave function in the Ising model, (ii) from the wave function in the Dicke model, (iii) from the correlation functions in the Dicke model. It is seen that all three measures reflect the π jumps related to the Rabi oscillation, and are quantitatively close to the expected values ($|\varphi| = 5\pi/6$ and $\pi/6$ for $\tau = \Delta/3$). It should be noted, though, that in contrast to the flux through the triangle, the relative phase in the double-well is not a gauge-invariant quantity, and shifting the initial time within the shaking period would modify the phase.

Finally, we mention that, although we have not considered decoherence effects explicitly, we have checked that the dynamics are not significantly changed by an initial finite phonon population, therefore excluding RF heating due to trap imperfections or noisy electric fields

as possible decoherence sources. Thus, decoherence is mainly expected due to technical imperfections like laser beam pointing and intensity noise or uncompensated stark shifts.

In summary, we have simulated a system of three ions which encircle an artificial flux engineered by periodic driving. Our simulation not only has shown the feasibility of Floquet engineering in trapped ions, but also revealed an unexpected robustness of the spin dynamics when the driving breaks time-reversal symmetry in the effective model. This effect could stabilize and further enhance the quantum simulation of topological models also in larger systems. Having shown a path towards complex-valued spin-spin interaction, we believe that trapped ions provide an ideal system for studying the role of topology and topological protection in small clusters with tunable system sizes from microscopic to mesoscopic regimes. Potentially, such clusters will provide robust building blocks for larger quantum devices.

ACKNOWLEDGMENTS

We are grateful to Alexey Gorshkov, Christopher Monroe, Bruno Julía-Díaz, Jiehang Zhang, Paul Hess, and Zhexuan Gong for interesting discussions. Financial support from AFOSR-MURI, EU grants EQuaM (FP7/2007-2013 Grant No. 323714), OSYRIS (ERC-2013-AdG Grant No. 339106), SIQS (FP7-ICT-2011-9 No. 600645), QUIC (H2020-FETPROACT-2014 No. 641122), Spanish MINECO (SEVERO OCHOA Grant SEV-2015-0522, FISICATEAMO FIS2016-79508-P), the Generalitat de Catalunya (SGR 874 and CERCA program), Fundacio Privada Cellex is acknowledged. GP is supported by the IC postdoctoral Research Fellowship program.

[1] Y. Aharonov and D. Bohm, Phys. Rev. **115**, 485 (1959).
[2] A. Shapere and F. Wilczek, *Geometric Phases in Physics*, Advanced Series in Mathematical Physics Vol. 5 (World Scientific, 1989).
[3] D. R. Hofstadter, Phys. Rev. B **14**, 2239 (1976).
[4] M. Janssen, O. Viehweger, U. Fastenrath, and J. Hajdu, *Introduction to the Theory of the Integer Qunantum Hall Effect* (Wiley, John and Sons, 1994).
[5] R. B. Laughlin, Phys. Rev. Lett. **50**, 1395 (1983).
[6] X. Wen, *Quantum Field Theory of Many-Body Systems*, Oxford Graduate Texts (OUP Oxford, 2004).
[7] C. Nayak, S. H. Simon, A. Stern, M. Freedman, and S. Das Sarma, Rev. Mod. Phys. **80**, 1083 (2008).
[8] J. Struck, C. Ölschläger, M. Weinberg, P. Hauke, J. Simonet, A. Eckardt, M. Lewenstein, K. Sengstock, and P. Windpassinger, Phys. Rev. Lett. **108**, 225304 (2012).
[9] H. Miyake, G. A. Siviloglou, C. J. Kennedy, W. C. Burton, and W. Ketterle, Phys. Rev. Lett. **111**, 185302 (2013).
[10] M. Aidelsburger, M. Atala, M. Lohse, J. T. Barreiro, B. Paredes, and I. Bloch, Phys. Rev. Lett. **111**, 185301 (2013).
[11] G. Jotzu, M. Messer, R. Desbuquois, M. Lebrat, T. Uehlinger, D. Greif, and T. Esslinger, Nature **515**, 237 (2014).
[12] M. Mancini, G. Pagano, G. Cappellini, L. Livi, M. Rider, J. Catani, C. Sias, P. Zoller, M. Inguscio, M. Dalmonte, and L. Fallani, Science **349**, 1510 (2015).
[13] B. K. Stuhl, H.-I. Lu, L. M. Aycock, D. Genkina, and I. B. Spielman, Science **349**, 1514 (2015).
[14] F. Meinert, M. J. Mark, K. Lauber, A. J. Daley, and H.-C. Nägerl, Phys. Rev. Lett. **116**, 205301 (2016).
[15] M. Hafezi, S. Mittal, J. Fan, A. Migdall, and J. Taylor, Nat. Photon. **7**, 1001 (2013).
[16] N. Schine, A. Ryou, A. Gromov, A. Sommer, and J. Simon, Nature **534**, 671 (2016).
[17] P. Roushan *et al.*, Nat. Phys. **13**, 146 (2017).
[18] P. Lodahl, S. Mahmoodian, S. Stobbe, A. Rauschenbeutel, P. Schneeweiss, J. Volz, H. Pichler, and P. Zoller, Nature **541**, 473 (2017).
[19] F. Kong, C. Ju, Y. Liu, C. Lei, M. Wang, X. Kong, P. Wang, P. Huang, Z. Li, F. Shi, L. Jiang, and J. Du, Phys. Rev. Lett. **117**, 060503 (2016).
[20] F. Mintert and C. Wunderlich, Phys. Rev. Lett. **87**, 257904 (2001).
[21] D. Porras and J. I. Cirac, Phys. Rev. Lett. **92**, 207901 (2004).
[22] A. Friedenauer, H. Schmitz, J. T. Glueckert, D. Porras, and T. Schaetz, Nat. Phys. **4**, 757 (2008).
[23] K. Kim, M.-S. Chang, R. Islam, S. Korenblit, L.-M. Duan, and C. Monroe, Phys. Rev. Lett. **103**, 120502 (2009).
[24] K. Kim, M. S. Chang, S. Korenblit, R. Islam, E. E. Edwards, J. K. Freericks, G. D. Lin, L. M. Duan, and C. Monroe, Nature **465**, 590 (2010).
[25] P. Richerme, Z.-X. Gong, A. Lee, C. Senko, J. Smith, M. Foss-Feig, S. Michalakis, A. V. Gorshkov, and C. Monroe, Nature **511**, 198 (2014).
[26] P. Jurcevic, B. P. Lanyon, P. Hauke, C. Hempel, P. Zoller, R. Blatt, and C. F. Roos, Nature **511**, 202 (2014).
[27] J. W. Britton, B. C. Sawyer, A. C. Keith, C.-C. J. Wang, J. K. Freericks, H. Uys, M. J. Biercuk, and J. J. Bollinger, Nature **484**, 489 (2012).
[28] J. G. Bohnet, B. C. Sawyer, J. W. Britton, M. L. Wall, A. M. Rey, M. Foss-Feig, and J. J. Bollinger, Science **352**, 1297 (2016).
[29] J. Zhang, G. Pagano, P. W. Hess, A. Kyprianidis, P. Becker, H. Kaplan, A. V. Gorshkov, Z.-X. Gong, and C. Monroe, ArXiv e-prints (2017), arXiv:1708.01044 [quant-ph].
[30] H. C. Nägerl, D. Leibfried, H. Rohde, G. Thalhammer, J. Eschner, F. Schmidt-Kaler, and R. Blatt, Phys. Rev. A **60**, 145 (1999).
[31] J. Smith, A. Lee, P. Richerme, B. Neyenhuis, P. W. Hess, P. Hauke, M. Heyl, D. A. Huse, and C. Monroe, Nat Phys **12**, 907 (2016).
[32] C. F. Roos, M. Riebe, H. Häffner, W. Hänsel, J. Benhelm, G. P. T. Lancaster, C. Becher, F. Schmidt-Kaler, and

R. Blatt, Science **304**, 1478 (2004).
[33] P. Jurcevic, H. Shen, P. Hauke, C. Maier, T. Brydges, C. Hempel, B. P. Lanyon, M. Heyl, R. Blatt, and C. F. Roos, ArXiv e-prints (2016), arXiv:1612.06902 [quant-ph].
[34] T. Graß, C. Muschik, A. Celi, R. W. Chhajlany, and M. Lewenstein, Phys. Rev. A **91**, 063612 (2015).
[35] D. H. Dunlap and V. M. Kenkre, Phys. Rev. B **34**, 3625 (1986).
[36] F. Grossmann, T. Dittrich, P. Jung, and P. Hänggi, Phys. Rev. Lett. **67**, 516 (1991).
[37] M. Holthaus, Phys. Rev. Lett. **69**, 351 (1992).
[38] M. Holthaus and D. Hone, Phys. Rev. B **47**, 6499 (1993).
[39] A. Eckardt, C. Weiss, and M. Holthaus, Phys. Rev. Lett. **95**, 260404 (2005).
[40] A. Eckardt, P. Hauke, P. Soltan-Panahi, C. Becker, K. Sengstock, and M. Lewenstein, EPL (Europhysics Letters) **89**, 10010 (2010).
[41] H. Lignier, C. Sias, D. Ciampini, Y. Singh, A. Zenesini, O. Morsch, and E. Arimondo, Phys. Rev. Lett. **99**, 220403 (2007).
[42] J. Struck, C. Ölschläger, R. Le Targat, P. Soltan-Panahi, A. Eckardt, M. Lewenstein, P. Windpassinger, and K. Sengstock, Science **333**, 996 (2011).
[43] T. Kitagawa, E. Berg, M. Rudner, and E. Demler, Phys. Rev. B **82**, 235114 (2010).
[44] L. Jiang, T. Kitagawa, J. Alicea, A. R. Akhmerov, D. Pekker, G. Refael, J. I. Cirac, E. Demler, M. D. Lukin, and P. Zoller, Phys. Rev. Lett. **106**, 220402 (2011).
[45] N. H. Lindner, G. Refael, and V. Galitski, Nat. Phys. **7**, 490 (2011), 10.1038/nphys1926.
[46] A. Bermudez, T. Schaetz, and D. Porras, Phys. Rev. Lett. **107**, 150501 (2011).
[47] T. Graß, M. Lewenstein, and A. Bermudez, New Journal of Physics **18**, 033011 (2016).
[48] C.-C. J. Wang and J. K. Freericks, Phys. Rev. A **86**, 032329 (2012).
[49] M. L. Wall, A. Safavi-Naini, and A. M. Rey, Phys. Rev. A **95**, 013602 (2017).
[50] Here, for simplicity we have assumed B_0 sufficiently larger than the Ising couplings J_{ij} such that the net effect of driving is equivalent to the driving of a XX model by the time-dependent magnetic field H_{B1}. More generally, the condition to achieve an effective XX model with the complex coupling as in Eq. (2) is $\int_0^{\tilde{T}} \exp[2i(2B_0t+\mu_i(t)+\mu_j(t))] = 0$, where $\tilde{T}$ is the period of $B_0t+\mu_i(t)$.